

Contribution from the Departments of Chemistry,
Concordia University, and McGill University, Montreal, Quebec, Canada

Arene Activation in Chromium Chalcocarbonyl Complexes. 1. Crystal and Molecular Structure of $\text{Cr}(\text{CO})_2(\text{CS})[(\text{CH}_3\text{O})_3\text{P}]_3$

PETER H. BIRD,[†] ASHRAF A. ISMAIL,[†] and IAN S. BUTLER*[‡]

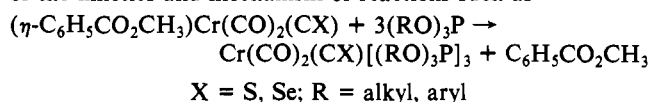
Received October 16, 1984

Reaction of $(\eta\text{-C}_6\text{H}_5\text{CO}_2\text{CH}_3)\text{Cr}(\text{CO})_2(\text{CS})$ with excess $(\text{CH}_3\text{O})_3\text{P}$ in toluene at 65 °C for 12 h results in replacement of the arene, and yellow crystals of $\text{Cr}(\text{CO})_2(\text{CS})[(\text{CH}_3\text{O})_3\text{P}]_3$ can be isolated in high purity. FT-IR and NMR (¹H, ¹³C, ³¹P) spectra suggest that the product has octahedral *mer* stereochemistry (with the two CO groups trans to each other) rather than the initially expected *fac* geometry. This molecular arrangement has been confirmed by room-temperature, single-crystal, three-dimensional X-ray diffraction: orthorhombic space group (D_{2h}^{15} , *Pbca*, $Z = 8$), $a = 15.61$ (1) Å, $b = 15.32$ (2) Å, $c = 18.88$ (1) Å, $V = 4505$ Å³, mol wt = 524, $\rho(\text{calcd}) = 1.47$ g cm⁻³, $\rho(\text{obsd}) = 1.40$ g cm⁻³; $R_F = 0.051$ and $R_{wF} = 0.073$ based on 1453 reflections with $I > 3\sigma(I)$. The Cr-(CS) bond is significantly shorter [1.782 (9) Å] than the two Cr-(CO) bonds [mean value 1.839 (9) Å], while the Cr-P bond trans to CS is appreciably longer [2.346 (3) Å] than the other two Cr-P bonds [mean value 2.262 (3) Å]. These variations in bond lengths are attributed to the stronger electron-withdrawing capacity of the CS ligand compared to that of CO.

Introduction

Transition-metal thiocarbonyl complexes often exhibit quite remarkable differences in chemical reactivity when compared to their carbonyl counterparts. Striking examples of this are the labilizing effects of the CS ligand in such reactions as CO substitution in $\text{W}(\text{CO})_5(\text{CS})^1$ and olefin substitution in $(\eta\text{-C}_5\text{H}_5)\text{-Mn}(\text{CO})(\text{CS})(\text{C}_8\text{H}_{14})^2$. More recently, the synthesis of $\text{Cr}(\text{C}-\text{O})_5(\text{CS})$ from $(\eta\text{-arene})\text{Cr}(\text{CO})_2(\text{CS})$ (arene = C_6H_6 , $\text{C}_6\text{H}_5\text{C}-\text{O}_2\text{CH}_3$, etc.) under moderate CO pressure has revealed the much greater lability of the arene rings in these complexes compared to those in the corresponding tricarbonyl analogues.³ Arene activation is even more pronounced in the related selenocarbonyl derivatives, $(\eta\text{-arene})\text{Cr}(\text{CO})_2(\text{CSe})^4$. All these various observations have been attributed to the much stronger electron-withdrawing capacities of the CS and CSe ligands compared to that of CO, leading to a decrease in the amount of $d\pi$ electron density being transferred from the metal center to the other π -acceptor ligands present in the complexes.⁵

In an effort to assess quantitatively the labilizing effects of the chalcocarbonyl ligands CS and CSe, we recently initiated a study of the kinetics and mechanism of reactions such as



Any information obtainable on the mechanism of this type of reaction will be of particular interest since, while arene activation is believed to be the prime factor in the catalytic hydrogenation of dienes using $(\eta\text{-arene})\text{Cr}(\text{CO})_3$ complexes,⁶ $(\eta\text{-arene})\text{Cr}(\text{CO})_2(\text{CS})$ complexes do not exhibit any catalytic activity.⁷ During the course of our kinetic investigation, it became crucial to identify the geometrical structure of the organometallic products. We report here the spectroscopic properties and the crystal and molecular structure of a typical product, $\text{Cr}(\text{CO})_2(\text{CS})[(\text{CH}_3\text{O})_3\text{P}]_3$.

Experimental Section

All synthetic reactions were performed under an atmosphere of pre-purified nitrogen. Toluene was freshly distilled over sodium strips under nitrogen. Trimethyl phosphite (Aldrich Chemical Co., Gold Label +99%) was used as obtained. $(\eta\text{-C}_6\text{H}_5\text{CO}_2\text{CH}_3)\text{Cr}(\text{CO})_2(\text{CS})$ was prepared by the literature method.³ FT-IR spectra were recorded on a Nicolet 6000 spectrometer (32 scans, 1-cm⁻¹ resolution). Proton and ³¹P NMR spectra were measured on a Varian XL-200 spectrometer equipped with a broad-band probe; ¹³C NMR spectra were measured on a Varian XL-300 spectrometer equipped with a 5-mm broad-band probe. The chemical shifts reported here are relative to Me_4Si (¹H and ¹³C) and $(\text{CH}_3\text{O})_3\text{P}$ (³¹P).

Preparation of $\text{Cr}(\text{CO})_2(\text{CS})[(\text{CH}_3\text{O})_3\text{P}]_3$. $(\eta\text{-C}_6\text{H}_5\text{CO}_2\text{CH}_3)\text{Cr}(\text{CO})_2(\text{CS})$ (200 mg, 0.69 mmol) was dissolved in toluene (25 mL).

Table I. Crystallographic Data for X-ray Diffraction Study of $\text{Cr}(\text{CO})_2(\text{CS})[(\text{CH}_3\text{O})_3\text{P}]_3$

Crystal Parameters	
cryst system: orthorhombic	$Z = 8$
space group: <i>Pbca</i>	$d_{\text{calcd}} = 1.466$ g cm ⁻³
$a = 15.61$ (1) Å	$d_{\text{obsd}} = 1.40$ (2) g cm ⁻³
$b = 15.32$ (2) Å	temp = 22 °C
$c = 18.88$ (1) Å	formula = $\text{C}_{12}\text{H}_{27}\text{O}_{11}\text{SP}_3\text{Cr}$
$V = 4505$ Å ³	mol wt = 524.0
Measurement of Intensity Data	
diffractometer: Picker Nuclear FACS-1	
radiation: Mo K α	
monochromator: highly oriented graphite	
detector aperture: 3 mm \times 3 mm	
cryst to detector dist: 25 cm	
detector: scintillation counter and pulse-height analyzer	
set for 100% of Mo K α peak	
attenuators: Ni foil used for intens $> 10^4$ Hz	
scan type: coupled $\theta(\text{cryst}) - 2\theta(\text{detector})$, 2.0° min ⁻¹	
scan length: $2\theta = [1.8 + (0.692 \tan \theta)]^\circ$, beginning 0.9°	
below the predicted peak	
rotation axis: [010]	
reflens measd: $+h, +k, +l$	
min and max 2θ : 3.5°, 40.0°	
stds every 50 cycles: 430, 006, 043	
variation: $\pm 3\%$ (random)	
no. of reflens collcd: 2108	
no. of reflens with $I > 3\sigma(I)$: 1453	
$R_F = 0.051$	
$R_{wF} = 0.073$	
GOF = 1.19	

$(\text{CH}_3\text{O})_3\text{P}$ (1.5 mL, 12.7 mmol) was added, and the reaction mixture was heated for 12 h at 65 °C. After the solution was allowed to cool to room temperature, all volatile material was removed under reduced pressure on a rotary evaporator. The remaining yellow solid was purified by preparative TLC on silica gel plates (eluent 3:2 dichloroethane-hexane). Yield: 311 mg (85%). Anal. Calcd for $\text{C}_{12}\text{H}_{27}\text{O}_{11}\text{P}_3\text{SCr}$: C, 27.6; H, 5.19; P, 17.7. Found (Guelph Chemical Laboratories): C, 27.2; H, 5.15; P, 17.0. FT-IR (KBr): $\nu(\text{CO})$ 1961 w, 1896 vs cm⁻¹; $\nu(\text{CS})$ 1205 cm⁻¹. ¹H NMR (CD_2Cl_2): 3.40 (d, $J = 11$ Hz, 1H), 3.72 ppm (d, $J = 11$ Hz, 2H). ¹³C NMR (CD_2Cl_2): 224.2 (q, $J = 22$ Hz, 2 CO), 336.5 ppm (td, $J_t = 30$ Hz, $J_d = 6$ Hz, CS). ³¹P NMR (CD_2Cl_2): 34.55 (t, $J = 63$ Hz,

- (1) Dombek, B. D.; Angelici, R. J. *Inorg. Chem.* **1976**, *15*, 1089.
- (2) Butler, I. S.; Fenster, A. E. *Inorg. Chim. Acta* **1973**, *7*, 79.
- (3) English, A. M.; Plowman, K. R.; Baibich, I. M.; Hickey, J. P.; Butler, I. S.; Jaouen, G.; Le Maux, P. *J. Organomet. Chem.* **1981**, *205*, 177.
- (4) English, A. M.; Plowman, K. R.; Butler, I. S.; Jaouen, G.; Le Maux, P.; Thépôt, J.-Y. *J. Organomet. Chem.* **1977**, *132*, C1.
- (5) Butler, I. S. *Acc. Chem. Res.* **1977**, *10*, 359.
- (6) Cais, M.; Frankel, D.; Weidenbaum, K. *Coord. Chem. Rev.* **1975**, *16*, 27.
- (7) Dabard, R.; Jaouen, G.; Simonneaux, G.; Cais, M.; Kohn, D. H.; Lapid, L.; Tatarsky, D. *J. Organomet. Chem.* **1980**, *184*, 91.

[†] Concordia University.

[‡] McGill University.

Table II. Final Positional Parameters for $\text{Cr}(\text{CO})_2(\text{CS})[(\text{CH}_3\text{O})_3\text{P}]_3$ and Their Estimated Standard Deviations

atom	<i>x</i>	<i>y</i>	<i>z</i>	<i>B</i> _{iso} ^a , Å ²
Cr	0.19911 (9)	0.38303 (9)	0.38742 (7)	2.43 (7)
P(1)	0.32792 (15)	0.41733 (16)	0.43546 (12)	2.82 (11)
P(2)	0.23895 (15)	0.44281 (15)	0.27786 (12)	2.67 (11)
P(3)	0.07087 (15)	0.33602 (16)	0.34657 (13)	2.81 (11)
C(1)	0.1663 (5)	0.3483 (5)	0.4733 (5)	2.9 (4)
S	0.13294 (20)	0.32226 (20)	0.54977 (14)	5.17 (15)
C(2)	0.2478 (6)	0.2782 (6)	0.3610 (5)	3.1 (4)
O(2)	0.2780 (5)	0.2140 (4)	0.3418 (4)	5.6 (4)
C(3)	0.1580 (6)	0.4919 (6)	0.4097 (5)	3.0 (4)
O(3)	0.1317 (4)	0.5600 (4)	0.4251 (4)	4.8 (4)
O(11)	0.3437 (4)	0.5118 (4)	0.4690 (3)	3.8 (3)
C(11)	0.3014 (7)	0.5356 (8)	0.5336 (6)	6.0 (6)
O(12)	0.4058 (4)	0.4123 (4)	0.3830 (3)	3.5 (3)
C(12)	0.4958 (6)	0.4274 (7)	0.4062 (6)	5.2 (6)
O(13)	0.3613 (4)	0.3626 (4)	0.5018 (4)	4.5 (3)
C(13)	0.3648 (7)	0.2686 (7)	0.4986 (7)	6.0 (6)
O(21)	0.2931 (4)	0.3858 (4)	0.2242 (3)	4.0 (3)
C(21)	0.2585 (7)	0.3154 (6)	0.1832 (5)	4.9 (6)
O(22)	0.2993 (4)	0.5250 (4)	0.2876 (3)	3.6 (3)
C(22)	0.3387 (7)	0.5691 (7)	0.2268 (5)	5.1 (6)
O(23)	0.1675 (4)	0.4755 (4)	0.2239 (3)	3.7 (3)
C(23)	0.1101 (7)	0.5445 (7)	0.2413 (6)	5.1 (6)
O(31)	-0.0097 (4)	0.4015 (4)	0.3464 (3)	4.0 (3)
C(31)	-0.0444 (7)	0.4313 (7)	0.4122 (6)	5.4 (6)
O(32)	-0.0238 (4)	0.2580 (4)	0.3858 (3)	3.9 (3)
C(32)	0.0672 (7)	0.1753 (7)	0.4016 (6)	5.2 (6)
O(33)	0.0683 (4)	0.3071 (4)	0.2664 (3)	3.6 (3)
C(33)	-0.0101 (6)	0.2719 (7)	0.2333 (5)	4.5 (6)

^a*B*_{iso} is the arithmetic mean of the principal axes of the thermal ellipsoid.

1P, 43.64 ppm (d, *J* = 63 Hz, 2P).

X-ray Data Collection, Structure Solution, and Refinement. The unit cell and data collection parameters are summarized in Table I. Weissenberg and precession photographs showed *mmm* symmetry and the following systematic absences, which uniquely define the space group *Pbca* (No. 61, *D*_{2h}¹⁴): on *Ok*l, *k* = 2*n* + 1; on *h*0*l*, *l* = 2*n* + 1; on *h**k*0, *h* = 2*n* + 1. The accurate unit cell dimensions were obtained by automatic centering of 51 reflections scattered randomly in reciprocal space in the range 15° < 2θ < 25°. The following formulas were used in the data reduction:

$$I = N - B(t_s/t_b) \quad \sigma(I) = [N + B(t_s/t_b)^2]^{1/2}$$

$$Lp = (\sin 2\theta)(\cos^2 2\theta_m + 1) / (\cos^2 2\theta + \cos^2 2\theta_m)$$

The net intensity *I* is derived from the total count *N* accumulated during the scan time *t_s*. The background count *B* was measured for time *t_b*. The Lorentz-polarization correction *Lp* is calculated for diffraction angles 2θ_m and 2θ_s at the monochromator and sample crystals, respectively.

The structure was solved by conventional heavy-atom techniques and refined by using the block-diagonal least-squares approximation. In the last stages of the refinement all atoms were refined with anisotropic thermal parameters. A final difference Fourier map was devoid of significant features; the highest peaks were about 1% of the intensity for the last carbon atom found and were randomly located. Also, since there appeared to be no clear indication of hydrogen atom locations, these atoms were not included in the structure factor calculations.

The computer programs used for the data collection, structure solution, and refinement and geometry calculations are those contained in the NRC PDP-8e crystallographic package.⁸ The perspective diagram was prepared by the Concordia University CDC Cyber system. The function minimized in the least-squares refinement was

$$\sum w(|F_o| - |F_c|)^2 \quad w = 1 / [(\sigma(F))^2 + 0.03F^2]$$

The discrepancy indices listed in Table I are

$$R_F = \sum ||F_o| - |F_c|| / \sum |F_o|$$

$$R_{wF} = [\sum w(|F_o| - |F_c|)^2 / \sum |F_o|^2]^{1/2}$$

$$\text{GOF} = [\sum w(|F_o| - |F_c|)^2 / (m - n)]^{1/2}$$

(8) Gabe, E. J.; Larson, A. C.; Lee, F. L.; Wang, Y. "The NRC PDP-8e Crystal Structure System"; NRC: Ottawa, Ontario, Canada, 1979.

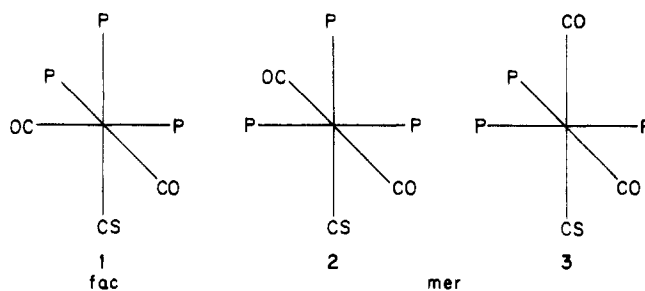


Figure 1. Possible isomers of $[(\text{CH}_3\text{O})_3\text{P}]_3\text{Cr}(\text{CO})_2(\text{CS})$.

The neutral-atom scattering factors and anomalous dispersion corrections were taken from standard tables.⁹ Listings of the observed and calculated structure factors are available; see the note on supplementary material at the end of this paper. The final atomic parameters are collected together in Table II.

Results and Discussion

The complex reported here, $\text{Cr}(\text{CO})_2(\text{CS})[(\text{CH}_3\text{O})_3\text{P}]_3$, is the first example of a substituted group 6²² metal thiocarbonyl complex containing more than one monodentate ligand other than CO. Attempts to prepare such complexes from $\text{Cr}(\text{CO})_5(\text{CS})$ by thermal replacement of the CO groups have only resulted in the loss of the CS ligand following the first substitution step, i.e. yielding first $\text{Cr}(\text{CO})_4(\text{CS})\text{L}$ and then $\text{Cr}(\text{CO})_4\text{L}_2$.¹ Thus, arene substitution provides the first entry into multisubstituted complexes of the type $\text{Cr}(\text{CO})_2(\text{CS})\text{L}_3$.

Arene replacement in $(\eta\text{-arene})\text{M}(\text{CO})_3$ complexes affords *fac*- $\text{M}(\text{CO})_3\text{L}_3$ (*M* = Cr, *L* = CH_3CN ;¹⁰ *M* = Mo, *L* = $(\text{CH}_3\text{-O})_3\text{P}$, Cl_3P , Ph_2ClP , *n*- Bu_3P ;^{11,12} *M* = W, *L* = $(\text{CH}_3\text{O})_3\text{P}$).¹³ *fac*- $\text{Mo}(\text{CO})_3[(\text{CH}_3\text{O})_3\text{P}]_3$ has also been synthesized by the substitution of cycloheptatriene in $(\eta\text{-C}_7\text{H}_8)\text{Mo}(\text{CO})_3$ by $(\text{CH}_3\text{-O})_3\text{P}$.¹⁴ The stereochemistry of the *fac* isomers was established by the appearance of two strong $\nu(\text{CO})$ peaks in the IR spectra, in accord with the *C*_{3v} local symmetry of the $\text{M}(\text{CO})_3$ moiety [$\nu(\text{CO}) = a_1 + e$]. We, as well as others,¹⁵ have observed that cycloheptatriene displacement from $(\eta\text{-C}_7\text{H}_8)\text{Cr}(\text{CO})_3$ by $(\text{C-H}_3\text{O})_3\text{P}$ in refluxing methylcyclohexane affords a mixture of *fac*- and *mer*- $\text{Cr}(\text{CO})_3[(\text{CH}_3\text{O})_3\text{P}]_3$. Similar mixtures are obtained from the reactions of $(\eta\text{-arene})\text{Cr}(\text{CO})_3$ complexes with monodentate ligands at high temperatures, as evidenced by the appearance of a third $\nu(\text{CO})$ band and the splitting patterns in the ³¹P NMR spectra.¹⁵

While the reactions of the tricarbonyl complexes described above yield predominantly the *fac* isomer under the conditions employed here, the $\nu(\text{CO})$ region in the FT-IR spectrum of $\text{Cr}(\text{CO})_2(\text{CS})[(\text{CH}_3\text{O})_3\text{P}]_3$ with one very strong and one very weak band being observed is clearly at variance with the intensity pattern expected for the *fac* isomer. The spectrum of the latter should most likely resemble that of *fac*- $\text{Cr}(\text{CO})_3\text{L}_3$ with two strong peaks of comparable intensity. The very low intensity of the 1961-cm⁻¹ peak is immediately suggestive of the *mer* isomer shown below in Figure 1 in which the two CO groups are trans to each other. The *mer* stereochemistry is further indicated by the similarity of the ³¹P NMR spectrum to that of *mer*- $\text{Cr}(\text{CO})_3[(\text{CH}_3\text{O})_3\text{P}]_3$ in CD_2Cl_2 solution, even down to the ²*J*_{pp} couplings (63 Hz).¹⁶ The solitary ¹³C NMR resonance for the CO groups is evidence of the absence of isomer 3, and its appearance as a quartet is in accord with the splitting that would be predicted for isomer 2, assuming

(9) "International Tables for X-Ray Crystallography"; Kynoch Press: Birmingham, England, 1979; Vol. IV, Tables 2.28-2.31.

(10) Yagupsky, G.; Cais, M. *Inorg. Chim. Acta* **1975**, *12*, 127.
 (11) Pidcock, A.; Smith, J. D.; Taylor, B. W. *J. Chem. Soc. A* **1967**, 872.
 (12) Zingales, F.; Chiesa, A.; Basolo, F. *J. Am. Chem. Soc.* **1966**, *88*, 2707.
 (13) Pidcock, A.; Smith, J. D.; Taylor, B. W. *J. Chem. Soc. A* **1969**, 1604.
 (14) Pidcock, A.; Taylor, B. W. *J. Chem. Soc. A* **1969**, 877.
 (15) Mathieu, R.; Lenzi, M.; Poilblanc, R. *Inorg. Chem.* **1970**, *9*, 2030.
 (16) ²*J*_{pp} couplings for *mer*- $\text{Cr}(\text{CO})_3[(\text{CH}_3\text{O})_3\text{P}]_3$ were measured under the same conditions given for $[(\text{CH}_3\text{O})_3\text{P}]_3\text{Cr}(\text{CO})_3(\text{CS})$ in the Experimental Section.

Table III. Bond Angles for $\text{Cr}(\text{CO})_2(\text{CS})[(\text{CH}_3\text{O})_3\text{P}]_3$ (deg) with Esd's in Parentheses

Angles about Chromium Atom			
Cis Angles			
C(1)–Cr–C(2)	96.0 (4)	C(2)–Cr–P(3)	89.7 (3)
C(1)–Cr–C(3)	87.8 (4)	C(3)–Cr–P(1)	90.4 (3)
C(1)–Cr–P(1)	87.6 (3)	C(3)–Cr–P(2)	86.6 (3)
C(1)–Cr–P(3)	87.8 (3)	C(3)–Cr–P(3)	93.4 (3)
C(2)–Cr–P(1)	86.9 (3)	P(1)–Cr–P(2)	91.6 (1)
C(2)–Cr–P(2)	89.6 (3)	P(2)–Cr–P(3)	93.3 (1)
Trans Angles			
C(1)–Cr–P(2)	174.4 (3)	P(1)–Cr–P(3)	174.0 (1)
C(2)–Cr–C(3)	175.2 (4)		
Angles in Cr–C(X) Linkages			
Cr–C(1)–S	176.4 (6)	Cr–C(3)–O(3)	178.7 (8)
Cr–C(2)–O(2)	177.2 (8)		
Angles about Phosphorus Atoms			
Cr–P–O	111.4 (2)–	O–P–O	96.2 (3)–
	120.3 (2)		104.0 (3)
Angles about Oxygen Atoms in Phosphite Ligands			
P–O–C	119.5 (6)–124.1 (6)		

Table IV. Bond Lengths for $\text{Cr}(\text{CO})_2(\text{CS})[(\text{CH}_3\text{O})_3\text{P}]_3$ (Å) with Esd's in Parentheses

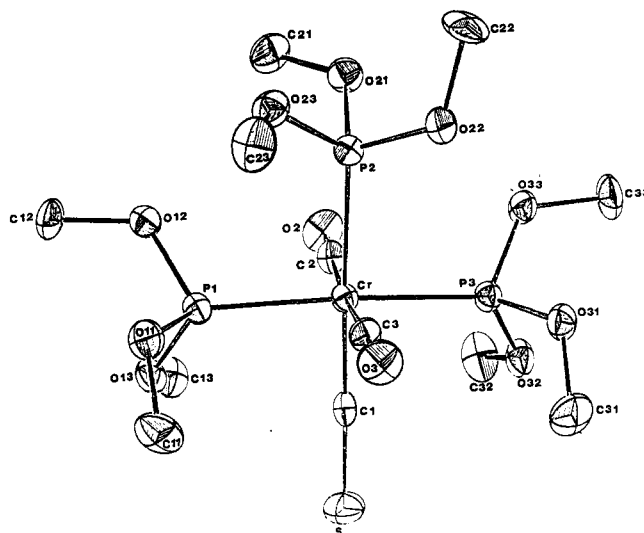
Cr–P(1)	2.265 (3)	C(1)–S	1.585 (9)
Cr–P(2)	2.346 (3)	C(2)–O(2)	1.148 (11)
Cr–P(3)	2.260 (3)	C(3)–O(3)	1.157 (11)
Cr–C(1)	1.782 (9)	P–O	1.569 (6)–1.607 (6)
Cr–C(2)	1.844 (9)	(P)O–C	1.424 (12)–1.488 (11)
Cr–C(3)	1.834 (9)		

that the two different tertiary phosphite environments are not sufficiently different to give rise to different values of $^2J_{\text{Cr}^{13}\text{C}-^{31}\text{P}}$. The observed coupling constant (22 Hz) is very close to the $^2J_{\text{Cr}^{13}\text{C}-^{31}\text{P}}$ value reported for $\text{Cr}(\text{CO})_5[(\text{CH}_3\text{O})_3\text{P}]$ and *trans*- $\text{Cr}(\text{CO})_4[(\text{CH}_3\text{O})_3\text{P}]_2$ (21 Hz).¹⁷ The ^{13}C S NMR resonance appears as a doublet, due to the unique ^{31}P – ^{13}C coupling, split into triplets by the other two equivalent ^{31}P nuclei, again in accord with isomer 2.

The *mer* stereochemistry (isomer 2) of the chromium thiocarbonyl derivative was confirmed by single-crystal X-ray diffraction (Table II). The resulting perspective diagram including the labeling scheme is shown in Figure 2. The arrangement of the ligands around the central Cr(0) atom is distorted from idealized octahedral geometry (see Table III for the interatomic angles). The OC–Cr–CO angle is 175.2 (4)°, while the *trans* phosphorus atoms are bent away from P(2) with P(1)–Cr–P(3) = 174.0 (1)°, presumably to minimize steric interactions between the three $(\text{CH}_3\text{O})_3\text{P}$ groups.

The interatomic distances are given in Table IV. The *trans* Cr–P bond lengths are equal within experimental error [mean value 2.262 (3) Å], while the Cr–P bond *trans* to CS is appreciably longer [2.346 (3) Å], i.e., an increase of 0.084 (3) Å. We attribute this to the strong electron-withdrawing capacity of the CS ligand, leading to a weakening (and lengthening) of the *trans* Cr–P bond.

A comparison of the Cr–C(S) and C–S bond lengths with those in related metal thiocarbonyl complexes containing terminal CS linkages¹⁸ reveals that these distances are among the longest C–S and shortest Cr–C(S) distances known. This effect is also reflected in the low value of the CS stretching frequency (1205 cm^{-1}). The Cr–C(S) bond distance is significantly shorter than the mean Cr–C(O) value [1.839 (9) Å]. We attribute these different observations to the relatively large amount of electron density available for π back-bonding at the metal center resulting from the presence of the three strongly σ -donating phosphite ligands. The variations observed in the bond distances associated with the

**Figure 2.** Perspective diagram of $[(\text{CH}_3\text{O})_3\text{P}]_3\text{Cr}(\text{CO})_2(\text{CS})$ showing 50% electron density probability ellipsoids.**Table V.** $\nu(\text{CS})$ Wavenumbers and C–S Bond Distances in Selected Transition-Metal Thiocarbonyl Complexes^a

complex	$\nu(\text{CS}), \text{cm}^{-1}$	$d(\text{C}-\text{S}), \text{Å}$
$[(\eta\text{-C}_5\text{H}_5)\text{Fe}(\text{CO})_2(\text{CS})]\text{PF}_6$	1348	1.501
$[\text{Ir}(\text{PPh}_3)_2(\text{CO})_2(\text{CS})]\text{PF}_6$	1321	1.511
$(\eta\text{-C}_5\text{H}_5)\text{Mn}(\text{CS})(\text{NO})(\text{I})$	1291	1.513
<i>trans</i> - $\text{RhCl}(\text{PPh}_3)_2(\text{CS})$	1299	1.536
$\text{Fe}(\text{OEP})(\text{CS})^b$	1292	1.559
<i>trans</i> - $\text{W}(\text{CO})_4(\text{CNC}_6\text{H}_{11})(\text{CS})$	1240	1.564
$(\eta\text{-C}_6\text{H}_4\text{CO}_2\text{CH}_3)\text{Cr}(\text{CO})_2(\text{CS})$	1225	1.570
$\text{Cr}(\text{CO})_2(\text{CS})[(\text{CH}_3\text{O})_3\text{P}]_3^c$	1205	1.585
$(\eta\text{-C}_{10}\text{H}_{10}\text{O})\text{Cr}(\text{CO})(\text{PPh}_3)(\text{CS})^d$		1.59
<i>cis</i> - $[(\eta\text{-C}_5\text{H}_5)\text{Fe}(\text{CO})(\text{CS})]_2$ (bridging thiocarbonyl ligands)	1124	1.592 1.587

^aData from: Woodard, S. S.; Jacobson, R. A.; Angelici, R. J. *J. Organomet. Chem.* **1976**, 117, C75, and references therein. ^bOEP = octaethylporphyrin, see: Scheidt, W. R.; Geiger, D. K. *Inorg. Chem.* **1982**, 21, 1208. ^cThis work. ^dKorp, J. D.; Bernal, I. *Cryst. Struct. Comm.* **1980**, 9, 821.

CS ligand are completely in accord with *ab initio* molecular orbital calculations for the free and coordinated CO and CS ligands: CS is expected to be a substantially better electron-withdrawing ligand than CO.¹⁹

Angelici has reported a linear relationship between the CS stretching frequency and the C–S bond length in a series of terminal thiocarbonyl complexes.¹⁸ Least-squares analysis of the currently available data given in Table V (excluding $\text{Fe}(\text{OEP})(\text{CS})$) yields a correlation coefficient of 0.99. Inclusion of $\text{Fe}(\text{OEP})(\text{CS})$ reduces the correlation significantly ($r = 0.94$). This may be attributed to appreciable mixing of $\nu(\text{CS})$ with $\nu[\text{M}-\text{C}(\text{S})]$, as observed in analogous porphinato thiocarbonyl complexes.²⁰

Conclusions

It has been shown in this study that arene displacement from $(\eta\text{-arene})\text{Cr}(\text{CO})_2(\text{CS})$ by $(\text{CH}_3\text{O})_3\text{P}$ yields predominantly²¹

(19) Saillard, J. Y.; Grandjean, D.; Caillet, P.; Le Beuze, A. *J. Organomet. Chem.* **1980**, 190, 371.

(20) Smith, P. D.; Dolphin, D.; James B. R. *J. Organomet. Chem.* **1981**, 208, 239.

(21) The FT-IR spectrum of the crude product of this reaction, prior to TLC purification, exhibits an additional peak in the carbonyl stretching region at 1957 cm^{-1} of weak intensity (<5% of that at 1896 cm^{-1}), which may be attributed to *fac*- $\text{Cr}(\text{CO})_2(\text{CS})[(\text{CH}_3\text{O})_3\text{P}]_3$ present in a very small amount. [The second $\nu(\text{CO})$ mode of this isomer is presumed to be hidden under the intense peak of the *mer* isomer at 1896 cm^{-1} .] This assignment has been verified during investigations of the isomerization of the *mer* isomer currently in progress in this laboratory.

(17) Bodner, G. M. *Inorg. Chem.* **1975**, 14, 2694.

(18) Woodward, S. S.; Jacobson, R. A.; Angelici, R. J. *J. Organomet. Chem.* **1976**, 117, C75.

$\text{Cr}(\text{CO})_2(\text{CS})[(\text{CH}_3\text{O})_3\text{P}]_3$ with octahedral *mer* stereochemistry. The CO groups are mutually trans, and the CS ligand is trans to one of the trimethyl phosphite ligands. The explanation for this stereochemical preference does not appear to originate with steric effects since $\text{Cr}(\text{CO})_3\text{L}_3$ complexes ($\text{L} = \text{THF}, \text{CH}_3\text{CN}, \text{R}_3\text{P}$), when synthesized under the same conditions as those employed here, are isolated as *fac* isomers even though they are significantly distorted due to steric effects. The formation of only

one of the two possible *mer* isomers of $\text{Cr}(\text{CO})_2(\text{CS})[(\text{CH}_3\text{O})_3\text{P}]_3$ further suggests that the stereochemical preference is dictated by the electronic properties of the thiocarbonyl ligand.

Acknowledgment. This work was generously supported by research grants from the NSERC (Canada) and the FCAC (Quebec). I.S.B. wishes to acknowledge the warm hospitality extended to him by the CNRS Laboratoire de Chimie de Coordination, Toulouse, and the Laboratoire de Cristalochimie, Université de Rennes I, while on sabbatical leave in France.

Registry No. $\text{Cr}(\text{CO})_2(\text{CS})[(\text{CH}_3\text{O})_3\text{P}]_3$, 97279-46-4; ($\eta\text{-C}_6\text{H}_5\text{CO}_2\text{CH}_3$) $\text{Cr}(\text{CO})_2(\text{CS})$, 52140-27-9; CS, 2944-05-0; C, 7440-44-0; S, 7704-34-9.

Supplementary Material Available: Listings of final thermal parameters, interatomic distances and angles, and structure factors (14 pages). Ordering information is given on any current masthead page.

- (22) In this paper the periodic group notation is in accord with recent actions by IUPAC and ACS nomenclature committees. A and B notation is eliminated because of wide confusion. Groups IA and IIA become groups 1 and 2. The d-transition elements comprise groups 3 through 12, and the p-block elements comprise groups 13 through 18. (Note that the former Roman number designation is preserved in the last digit of the new numbering: e.g., III \rightarrow 3 and 13.)

Contribution from the Departments of Chemistry, University of Canterbury, Christchurch, New Zealand, and University of Southern California, Los Angeles, California 90089-1062

Further Insight into Magnetostructural Correlations in Binuclear Copper(II) Species Related to Methemocyanin: X-ray Crystal Structure of a 1,2- μ -Nitrito Complex

VICKIE MCKEE,*¹ MARUTA ZVAGULIS,² and CHRISTOPHER A. REED*²

Received October 16, 1984

The X-ray crystal structure of the nitrite complex $[\text{Cu}_2(\text{L-Et})(\text{NO}_2)](\text{ClO}_4)_2$ (HL-Et = *N,N,N',N'*-tetrakis(2-(1-ethylbenzimidazolyl))-2-hydroxy-1,3-diaminopropane) has been determined as a further test of the hypothesis of $d_{x^2-y^2}/d_{z^2}$ orbital switching which was used to explain the markedly different magnetic properties of the analogous azide and acetate complexes. Crystal data: monoclinic, $P2_1/n$, $a = 14.229$ (3) Å, $b = 22.683$ (6) Å, $c = 15.913$ (4) Å, $\beta = 98.92^\circ$ (2), $Z = 4$. The copper(II) stereochemistries are close to trigonal bipyramidal with the alkoxide taking an equatorial bridging site. The nitrite ligand is asymmetrically bound, forming an O,N bridge between axial sites. Despite very close structural similarity to the ferromagnetic acetate complex ($2J = +24 \text{ cm}^{-1}$), the nitrite complex is quite strongly antiferromagnetically coupled ($2J = -278 \text{ cm}^{-1}$). This is traced to complementary symmetries of the bridging ligand orbitals. This concept of *ligand orbital complementarity* is also used to gain a deeper understanding of the diamagnetism of the azide complex $[\text{Cu}_2(\text{L-Et})(\text{N}_3)]^{2+}$. The relationship of these findings to the geometry and magnetic properties of methemocyanin and oxyhemocyanin is discussed.

Introduction

Although there is already a long history and a prolific literature on the subject of magnetic coupling in binuclear copper(II) complexes,³⁻⁷ a sustained interest remains.⁸ In part, this is because binuclear copper sites in proteins such as hemocyanin and laccase⁹ are notable examples of what still comprises only a handful of complexes¹⁰⁻¹⁴ that closely approach diamagnetism at room temperature. On the synthetic front, new series of complexes that

mimic the protein sites or relate the extent of magnetic coupling to detailed structural parameters continue to be discovered.¹⁴⁻²³ And at the same time, the conceptual understanding of magnetic coupling in terms of the interactions of magnetic orbitals continues to evolve.²⁴⁻²⁷ Unsymmetrically dibridged systems are, however, poorly understood.

- (1) University of Canterbury.
- (2) University of Southern California.
- (3) Hatfield, W. E. *ACS Symp. Ser.* **1975**, No. 5, 108.
- (4) Hodgson, D. J. *Prog. Inorg. Chem.* **1975**, *19*, 173-241.
- (5) Doedens, R. J. *Prog. Inorg. Chem.* **1976**, *21*, 209-231.
- (6) Sinn, E. *Inorg. Chem.* **1976**, *15*, 358-365.
- (7) Melnik, M. *Coord. Chem. Rev.* **1982**, *42*, 259-293.
- (8) Willet, R. D., Ed. "NATO ASI on Magneto-Structural Correlations in Exchange Coupled Systems"; Reidel: Amsterdam, 1984.
- (9) Dooley, D. M.; Scott, R. A.; Ellinghaus, J.; Solomon, E. J.; Gray, H. B. *Proc. Natl. Acad. Sci. U.S.A.* **1978**, *75*, 3019-3022.
- (10) Bertrand, J. A.; Smith, J. H.; Eller, P. G. *Inorg. Chem.* **1974**, *13*, 1649-1653.
- (11) DeCourcy, J. S.; Waters, T. N.; Curtis, N. F. *J. Chem. Soc., Chem. Commun.* **1977**, 572-573 and references therein.
- (12) Butcher, R. J.; O'Connor, C. J.; Sinn, E. *Inorg. Chem.* **1979**, *18*, 1913-1918.
- (13) Agnus, Y.; Louis, R.; Gisselbrecht, J.-P.; Weiss, R. *J. Am. Chem. Soc.* **1984**, *106*, 93-102 and references therein.
- (14) Sorrell, T. N. "Abstracts of Papers", Inorganic and Biochemical Perspectives in Copper Coordination Chemistry, Albany, NY, July 23-27, 1984, and accompanying presentation.

- (15) Thompson, L. K.; Hanson, A. W.; Ramaswamy, B. S. *Inorg. Chem.* **1984**, *23*, 2459-2465.
- (16) McKee, V.; Zvagulis, M.; Dagdigian, J. V.; Patch, M. G.; Reed, C. A. *J. Am. Chem. Soc.* **1984**, *106*, 4765-4772.
- (17) Kida, S.; Takeuchi, M.; Takahashi, K.; Nishida, Y. Abstracts, XXIII International Conference on Coordination Chemistry, Boulder, CO, July 29-Aug 3, 1984, and accompanying poster presentation.
- (18) Julve, M.; Verdager, M.; Kahn, O.; Gleizes, A.; Philoche-Levisalles, M. *Inorg. Chem.* **1983**, *22*, 368-370.
- (19) Comarmond, J.; Plumere, P.; Lehn, J.-M.; Agnus, Y.; Louis, R.; Weiss, R.; Kahn, O.; Morgenstern-Badarau, I. *J. Am. Chem. Soc.* **1982**, *104*, 6330-6340.
- (20) Timmons, J. H.; Martin, J. W. L.; Martell, A. E.; Rudolf, P.; Clearfield, A.; Loeb, S. J.; Willis, C. J. *Inorg. Chem.* **1981**, *20*, 181-186.
- (21) Hatfield, W. E. *Comments Inorg. Chem.* **1981**, *1*, 105-121.
- (22) Nishida, Y.; Takeuchi, M.; Takahashi, K.; Kida, S. *Chem. Lett.* **1983**, 1815-1818.
- (23) Fallon, G. D.; Murray, K. S.; Mazurek, W.; O'Connor, M. J. *Inorg. Chim. Acta* **1985**, *96*, L53-L55.
- (24) Hay, P. J.; Thibeault, J. C.; Hoffmann, R. *J. Am. Chem. Soc.* **1975**, *97*, 4884-4899.
- (25) Haddad, M. S.; Wilson, S. R.; Hodgson, D. J.; Hendrikson, D. N. *J. Am. Chem. Soc.* **1981**, *103*, 384-391.
- (26) Kahn, O. *Inorg. Chim. Acta*, **1982**, *62*, 3-14.
- (27) Kahn, O. *Comments Inorg. Chem.* **1984**, *3*, 105-132.